Photonic Micro-Electromechanical Systems Vibrating at *X*-band (11-GHz) Rates

Matthew Tomes and Tal Carmon*

Electrical Engineering and Computer Science, University of Michigan, Ann Arbor, Michigan 48109, USA
(Received 7 July 2008; published 19 March 2009)

We report on an opto-mechanical resonator with vibration excited by compressive radiation pressure via stimulated Brillouin scattering [SBS]. We experimentally excite a mechanical whispering-gallery mode (WGM) from an optical WGM and detect vibration via the red Doppler shifted (Stokes) light it scatters. We numerically solve the stress-strain equation to calculate the circumferentially circulating mechanical WGM and reveal mechanical WGMs with a variety of transverse shapes. Frequency in our device is limited by the shortest optical wavelength it can transmit, irrespective of device size.

Introduction.—Devices resonating optically as well as mechanically have demonstrated coupling between their mechanical mode and their electromagnetic mode via radiation pressure. Such solid devices were investigated both theoretically and experimentally [1–11].

Further, high frequency mechanical oscillators are attractive as local oscillators to support communication applications and atomic clocks [12] where frequencies comparable with the Caesium transition are attractive. Increasing vibration rates in micro-electromechanical systems [MEMS] is usually restricted by miniaturization. For instance, in cavities based on a moving cavity element [Fig. 1(b)] such as the walls of an optical whispering-gallery mode (WGM) cavity [13], a flexible mirror in a Fabry-Perot [14–18], and a flexible membrane [11], frequency is restricted by the time it takes sound to cross these elements. Relaxation of this condition was reported by using high-order modes that allow trading off GHz rates [19] for efficiency. Here, we excite a very high-order (~1000 nodes) mechanical WGM by using SBS. We replace traditional forces in photonic MEMS, such as centrifugal radiation pressure [13], with stimulated Brillouin scattering (SBS) induced compression. We experimentally demonstrate and theoretically calculate a mechanical WGM at 11 GHz excited by an optical WGM. This mechanical mode is probed optically via beating between the incoming light (pump) and the red Doppler shifted (Stokes) light scattered from the mechanical WGM.

Theory.—Optical WGMs circumferentially propagating in a sphere [20] are named after an acoustical analogue reported by Rayleigh in 1910. We calculate both an optical WGM [21] and an acoustical WGM for a 100-μm silica sphere [Fig. 1(a)]. The optical and mechanical WGMs have integer number of wavelengths along circumference so multiple recirculations interfere constructively (resonances). To calculate the mechanical WGM, we numerically solve the exact tensorial stress-strain equations, where the only assumption is discretization of space. Only longitudinal mechanical modes having acoustical wavelength half of the optical wavelength are taken into

account, as others modes are less likely to be excited by SBS [22,23]. Though the relevant mechanical modes are mostly longitudinal, our solver still accounts for transverse deformation occurring through the Poisson ratio. The acoustical wavelength is half the optical wavelength [22,23], and the mechanical-mode area (in the plane transverse to propagation) is smaller than an optical-wavelength square (calculated in Fig. 1). This allows the vibrating mass to be as low as 0.15 ng, which is much lighter than in prior photonic MEMS and allows low power consumption.

Knowing the forms of both the electromagnetic as well as the acoustic WGM, we can discuss their opto-mechanical interaction. A time-varying electric field gives rise to a time-varying electrostrictive strain [22]. The presence of a mechanical mode, on the other hand, photo-
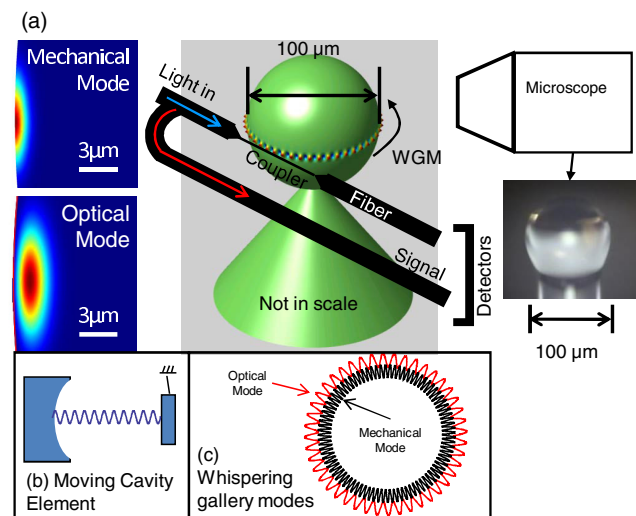

FIG. 1 (color online). (a) Left: Cross sectional views of the calculated mechanical and optical modes (stress and electric fields). Right: Experimental setup. (b) Illustration of a moving cavity element as in other photonic MEMS. (c) Illustration of our WGM cavity where the acoustical and optical modes are circumferentially circulating.

elastically changes the optical dielectric constant. Hence, it can cause exchange of energy between electromagnetic waves whose frequencies differ by an amount equal to the mechanical frequency. With sufficient pump intensity, there can be simultaneous generation of a counter-circulating optical WGM (named Stokes mode) and a co-circulating mechanical WGM at frequency $\Omega_m = \omega_p - \omega_s$, where ω_p and ω_s stand for the angular frequency of the optical pump and Stokes mode, respectively. The pump excites the mechanical vibration through a self-consistent process in which the two optical modes beat, and via the electrostrictive effect, apply stress to the material which drives the mechanical mode. In return, this mechanical mode, via the photo-elastic effect, writes a travelling optical grating that reflects and red Doppler shifts the optical pump into the Stokes mode ($\omega_s = \omega_p - \Omega_m$). Such a self-consistent interaction where the vibration as well as the counter-circulating Stokes mode are produced by the one optical input only [24] is called SBS. For satisfying phase match [22] and for benefiting from resonance enhancement in such a process, both optical frequencies should be cavity resonances, and the separation between them should be equal to the mechanical resonance frequency [22] as described by $\omega_s = \omega_p(1 - \frac{vn}{c})$. Here, v and c/n are the velocities of sound and light, respectively. We approximate these velocities as that of plane waves and calculate them more accurately with the numerical WGM solvers as in Fig. 1(a). The resulting optical-mode separation given for silica at telecom wavelength (1.5 μm) is approximately 11 GHz. An additional requirement is that the integer number of optical wavelengths resonating along circumference must be twice the number of acoustical wavelengths [22]. The first requirement ($\omega_s = \omega_p - \Omega_m$) is generally referred to as originating from energy conservation, while the second requirement originates from momentum conservation. In fibers and bulk materials, propagation of the ~11 GHz red-shifted Stokes light is guaranteed; however, in our micro-resonator, the approximately 300 GHz optical free-spectral-range restricts fundamental optical modes from being separated by 11 GHz. Luckily, using optical WGMs with high-order transverse profiles modifies the velocity of light. This recently allowed bringing optical modes very close to each other in frequency [25,26]. Thus, high-order optical modes can provide the required frequency separation of ~11 GHz. Further, we calculate that, analogous to the optical WGM [25,26], the acoustical WGM can have high-order transverse profiles [Fig. 3(b)]. This modifies the mechanical modes' velocities, v, and hence also varies their frequencies [Fig. 3(a)]. Thus, many mechanical modes are allowed, and the one with the $\Omega_m = \omega_p - \omega_s$ frequency will be excited. In our experiments, we observed resonators where almost every optical mode excites vibration, leading us to believe that the mechanical mode is selected from a continuity of modes.

As for required power, the stimulated Brillouin effect is analogous to stimulated Raman scattering with the mechanical mode playing the role of the molecular vibration [22,24]. We can write the self-excitation threshold as

$$P_{\text{threshold}} = \left(\frac{\pi^2 n^2 V}{B g \lambda_p \lambda_s Q_s Q_p}\right)\left(\frac{1}{1 + Q_m \lambda_m/2\pi r}\right). \quad (1)$$

Here, $P_{\text{threshold}}$ denotes the incident power required to excite mechanical vibrations. V is the optical-mode volume, B stands for the modal overlap, $Q_{p,s,m}$ are the quality factors of the pump, stokes, and mechanical modes, $\lambda_{p,s,m}$ are the wavelengths, r is the cavity radius, and g is the nonlinear bulk Brillouin gain coefficient [23]. The first fraction in Eq. (1) is similar to the one known for the Raman threshold in cavities as described in [27]. This first fraction includes the optical finesse (the number of times light recirculates the cavity) for the pump mode and describes the optical resonance enhancement via recirculations. High finesse is one important difference of our work from previous experiments, such as fibers resonators, which possess lower finesse and require higher power to excite SBS. The second fraction in Eq. (1) stands for mechanical resonance enhancement by acoustical recirculations. In a large resonator where $r \gg Q_m \lambda_m$, the second fraction is approximately one, describing no contribution of mechanical resonance enhancement. In our case, the recorded mechanical dissipation for silica [23] gives a mechanical quality factor of 770 [28]. At our cavity size, this suggests a reduction of threshold by a factor of 2.3. As for competition from other processes, Brillouin gain (g) is considerably larger than the gain of other processes in silica [23] (e.g., Rayleigh and Raman scattering); it is hence expected that Brillouin gain will dominate with proper phase matching.

Experiment.—Our experiment [Fig. 1(a)] uses a 100-μm diameter spherical WGM cavity [29] that is made out of a silica fiber via CO_2 laser reflow. The sphere exhibited an optical quality factor, Q_p, of 300×10^6 measured via the resonance width. Such spheres can also be made on-chip as described in [30,31]. A pump laser is fiber coupled [32,33] and thermally self locked [34] to an optical WG resonance, providing the power to drive the mechanical WGM. The signal is backward coupled while the pump is forward coupled as described in Fig. 1(a). This is possible because the two modes circulate in opposite directions. We therefore have the freedom to measure each output (Stokes signal or pump transmission) separately.

Frequency.—To show excitation of mechanical modes at X-band (11 GHz) rates, we measure the frequency with an electrical spectrum analyzer. Combining forward and backward outputs allows measuring mechanical frequency via the optical beat note between pump and Stokes signals. This is measured with a photodiode connected to an electrical spectrum analyzer. The measured frequency [Fig. 2(a)] deviates only 2% from the numerically calcu-

lated frequency (Fig. 1) for the mechanical mode. Such deviation is within the experimental error in measuring the size of our device. The width of this line is 0.7 MHz.

Optical spectrum.—We connect the backward coupler to an optical spectrum analyzer and measure the red-shifted Stokes line and the residual scattering of the pump [Fig. 2(b)]. The pump-Stokes separation is 11.5 GHz lying within the experimental error for our optical spectrum analyzer ($+-1$ GHz). The Stokes line being stronger than back scattering from the pump indicates that the Rayleigh back scattering is at least 1 order of magnitude smaller than our scattering from mechanical vibration. This is expected as the Brillouin gain is larger than the Rayleigh gain [23]. Figure 2(b) also indicates that the Stokes line is more than 5 orders of magnitude stronger than the noise level in our system.

Efficiency and threshold.—The output power of the Stokes signal is measured with a power meter while varying the input power [Fig. 2(c)]. Experimental results indicate a resulting slope efficiency of 90% and a 26 μW self-excitation threshold. During measurement, part of the light is continuously monitored with an optical spectrum analyzer to verify that the cavity is clean from other optical effects.

Acoustical mode spectroscopy.—Here, we used a 210 μm cavity, which has the advantage of allowing hundreds of modes around 10–11 GHz apart, each excited with a different optical wavelength. We move from one optical resonance to another by changing the laser wavelength, while recording the corresponding mechanical vibration frequency. The experimental results are given in Fig. 3(a). The overall trend in Fig. 3(a) is expected from the fact that the acoustical wavelength scales with the optical wavelength. One explanation for the variation in Fig. 3(a) can be

the calculated abundance of high-order mechanical WGMs, represented by lines in Fig. 3(a), and linked by an arrow to their corresponding stress field in Fig. 3(b). We note that in the past, the existence of such high-order optical modes was measured to relax phase match conditions and allow third-harmonic generation [30], making it likely that such mechanism exist also in the acoustical domain. The fact that some of calculated high-order mechanical WGMs in Fig. 3(a) better overlap spatially with a typical optical WGMs makes it likely that these high-order mechanical WGM explain the 400 MHz vibration variance.

Cascaded vibration modes.—In this experiment, we measure the optical spectrum at the forward and backward outputs. We measure that the opto-mechanical coupling in our system was strong enough to excite up to 3 cascaded mechanical modes simultaneously [Fig. 3(c)] with input power lower than 1 mW. Beat notes between such cascaded events should be approximately twice and 3 times the vibration rate (2×11 GHz and 3×11 GHz). As expected, we observe a beat note (between pump and the second Stokes line) at 22 GHz as shown in Fig. 3(d), which is near the highest frequency that our electrical spectrum analyzer can measure.

Conclusion.—We exploit SBS to drive a high frequency mechanical WGM in a silica resonator. Our MEMS is operating continuously in time at room temperature and pressure. The vibration is self-excited, and there is no need for external modulation or feedback. The difference from previous photonic MEMS is exciting much higher frequen-
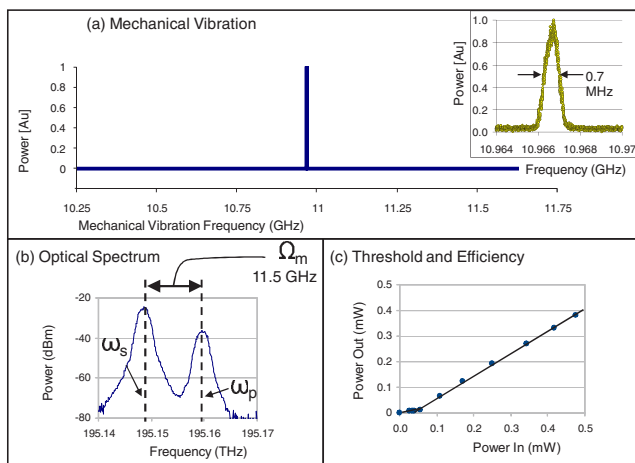

FIG. 2 (color online).   Experimental results. (a) Vibration readout from an electrical spectrum analyzer which is connected to a photodetector. (b) Readout from the optical spectrum analyzer showing both the Stokes line and the residual scattering of the pump, (c) Power out vs power in.
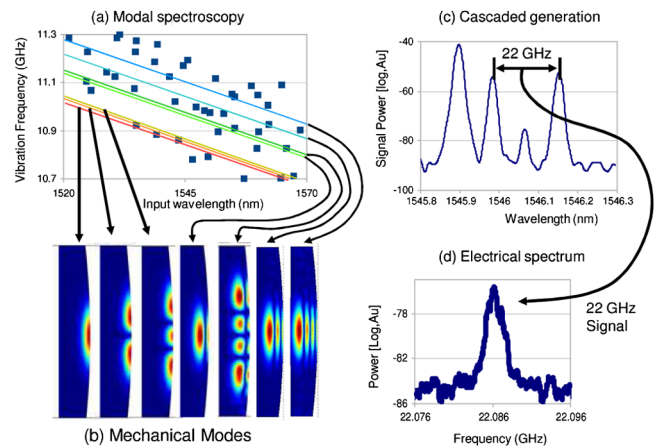

FIG. 3 (color online).   Experimental results. (a) Modal spectroscopy of the cavity. Mechanical frequency is experimentally obtained in a single cavity for many different optical wavelengths and plotted as points. Calculated mechanical modes are plotted as lines (actually consisting of points) linked with an arrow to their calculated stress field. (b) Stress fields of different mechanical modes representing the lines in (a). (c) Optical spectrum of the cascaded generation. (d) Electrical spectrum analyzer output showing 22 GHz beat note between the first and third cascaded generation of Stokes lines.

cies scaling inversely with optical wavelength. Additionally, unlike the breathing resonators where the Doppler shifted lines [13] were emitted together with the transmitted pump light, here, the Stokes and Pump signals are emerging from two separate fibers and will allow future studies where detection of the Stokes line and the pump should be done by two separated detectors.

The vibration in our resonator is azimuthal and not radial as in prior work [12,13,19]. Except for the geometrical difference, radial motion generally propagates toward the support and hence requires special mounting to prevent mechanical energy from leaking through the support [12]. While both the work in [12] and in here rely on electrostrictive pressure, in our work, the electric field of light drives vibration, replacing the electrical field applied by metal electrodes [12]. We believe that the continuous trend in improving UV lasers and the availability of material with fast velocity of sound will allow in future photonic-MEMS vibrating at even higher rates. Most attractive for high frequencies is diamond where available polishing techniques in crystals [35] allow high-Q resonators. Diamond will allow higher than 200 GHz rates if excited at the shortest optical wavelength it transmits well. Though our device is different, high frequency oscillations were exploited to improve signal/noise ratio in various experiments (for example, [36–38]), raising challenges such as making the measurement faster than phonon lifetime [39].

The authors acknowledge fruitful discussion with Ravi Hedge.

Note added.—Recently, Brillouin lasing with a CaF_2 whispering-gallery mode resonator was reported [40].

---

*To whom correspondence should be addressed:
tcarmon@umich.edu

[1] V. B. Braginskii, F. Y. Khalili, and K. S. Thorne, *Quantum Measurement* (Cambridge University Press, Cambridge [England]; New York, 1992).
[2] L. Hilico *et al.*, Appl. Phys. B **55**, 202 (1992).
[3] A. Heidmann, Y. Hadjar, and M. Pinard, Appl. Phys. B **64**, 173 (1997).
[4] S. Bose, K. Jacobs, and P. L. Knight, Phys. Rev. A **59**, 3204 (1999).
[5] V. Giovannetti, S. Mancini, and P. Tombesi, Europhys. Lett. **54**, 559 (2001).
[6] W. Marshall *et al.*, Phys. Rev. Lett. **91**, 130401 (2003).
[7] M. Pinard *et al.*, Europhys. Lett. **72**, 747 (2005).
[8] A. Ferreira, A. Guerreiro, and V. Vedral, Phys. Rev. Lett. **96**, 060407 (2006).
[9] S. Pirandola *et al.*, Phys. Rev. Lett. **97**, 150403 (2006).
[10] D. Vitali *et al.*, Phys. Rev. Lett. **98**, 030405 (2007).
[11] J. D. Thompson *et al.*, Nature (London) **452**, 72 (2008).
[12] C. T. C. Nguyen, IEEE Trans. Ultrason. Ferroelectr. Freq. Control **54**, 251 (2007).
[13] T. Carmon *et al.*, Phys. Rev. Lett. **94**, 223902 (2005).
[14] C. H. Metzger and K. Karrai, Nature (London) **432**, 1002 (2004).
[15] O. Arcizet *et al.*, Nature (London) **444**, 71 (2006).
[16] S. Gigan *et al.*, Nature (London) **444**, 67 (2006).
[17] D. Kleckner and D. Bouwmeester, Nature (London) **444**, 75 (2006).
[18] T. Corbitt *et al.*, Phys. Rev. Lett. **98**, 150802 (2007).
[19] T. Carmon and K. J. Vahala, Phys. Rev. Lett. **98**, 123901 (2007).
[20] J. W. Lord Rayleigh, Philos. Mag. **20**, 1001 (1910).
[21] M. Oxborrow, IEEE Trans. Microwave Theory Tech. **55**, 1209 (2007).
[22] A. Yariv, *Quantum Electronics* (Wiley, New York, 1975), pp. 491–497.
[23] R. W. Boyd, *Nonlinear Optics* (Academic Press, Amsterdam; Boston, 2008), pp. 429–468.
[24] R. Y. Chiao, B. P. Stoicheff, and C. H. Townes, Phys. Rev. Lett. **12**, 592 (1964).
[25] T. Carmon *et al.*, Phys. Rev. Lett. **100**, 103905 (2008).
[26] A. A. Savchenkov *et al.*, Phys. Rev. A **76**, 023816 (2007).
[27] S. M. Spillane, T. J. Kippenberg, and K. J. Vahala, Nature (London) **415**, 621 (2002).
[28] The mechanical Q is derived from the mechanical dissipation of silica, at 11 GHz and at room temperature as measured and presented in Ref. [23]. As for surface smoothness effects, our system is nanoscale smooth which make it likely that such scattering is small. Though the optical scattering in our system is very small, we do not cancel a possibility for some acoustical scattering.
[29] D. W. Vernooy *et al.*, Opt. Lett. **23**, 247 (1998).
[30] T. Carmon and K. J. Vahala, Nature Phys. **3**, 430 (2007).
[31] D. K. Armani *et al.*, Nature (London) **421**, 925 (2003).
[32] J. C. Knight *et al.*, Opt. Lett. **22**, 1129 (1997).
[33] M. Cai and K. Vahala, Opt. Lett. **26**, 884 (2001).
[34] T. Carmon, L. Yang, and K. J. Vahala, Opt. Express **12**, 4742 (2004).
[35] V. S. Ilchenko *et al.*, Phys. Rev. Lett. **92**, 043903 (2004).
[36] R. J. Schoelkopf *et al.*, Phys. Rev. Lett. **78**, 3370 (1997).
[37] K. C. Schwab and M. L. Roukes, Phys. Today **58**, No. 7, 36 (2005).
[38] A. Gaidarzhy *et al.*, Phys. Rev. Lett. **94**, 030402 (2005).
[39] K. C. Schwab *et al.*, Phys. Rev. Lett. **95**, 248901 (2005); A. Gaidarzhy *et al.*, *ibid.* **95**, 248902 (2005).
[40] I. S. Grudinin, A. B. Matsko, and L. Maleki, Phys. Rev. Lett. **102**, 043902 (2009).